Macromolecules

ARTICLE

pubs.acs.org/Macromolecules

Core−Shell Molecular Bottlebrushes with Helical Polypeptide Backbone: Synthesis, Characterization, and Solution Conformations

Haoyu Tang,[†] Yuanchao Li,[‡] Samuel H. Lahasky,[†] Sergei S. Sheiko,[‡] and Donghui Zhang*,[†]

[†]Department of Chemistry and Macromolecular Studies Group, Louisiana State University, Baton Rouge, Louisiana 70803, United States

[‡]Department of Chemistry, University of North Carolina at Chapel Hill, North Carolina 27599-3290, United States

Supporting Information

ABSTRACT: A series of core−shell molecular bottlebrushes with helical polypeptide backbone and polylactide-*b*-poly(ethylene glycol) block copolymer side chains [PPLG-*g*-(PLA-*b*-PEG)] have been synthesized via a grafting-to method. The structurally well-defined side chains with low molecular weight distribution (PDI < 1.03) have been synthesized by ring-opening polymerization (ROP) of DL-lactides using PEG-OH macroinitiator and $AlEt_3$ catalyst. Postpolymerization modification by esterification enables the quantitative installation of an alkynyl functionality at the block polymer chain ends. Grafting of alkynyl-terminated PLA-*b*-PEG onto poly(γ-azidopropyl-L-glutamate) (PAPLG) via copper-mediated [2 + 3] alkyne−azide 1,3-dipolar cycloaddition yields the targeted molecular bottlebrushes with high grafting density under mild conditions. A combination of the Langmuir−Blodgett (LB) technique with atomic force microscopy (AFM) has allowed for direct imaging of the synthesized molecular brushes and characterization of their molecular weight (MW) distribution. The imaged individual macromolecules demonstrate a wormlike conformation with an average length shorter than the contour length of the backbone. In agreement with the AFM observations, circular dichroism (CD) studies of PPLG-*g*-(PLA-*b*-PEG) in aqueous solution reveal that all molecular bottlebrushes retain backbones with α-helical conformations in acidic or neutral conditions. Longer side chains destabilize the helical conformations due to enhanced steric hindrance. Temperature variation can cause partial and reversible unfolding of the helical backbones. The temperature effect is greatly diminished for the bottlebrushes with longer side chains.

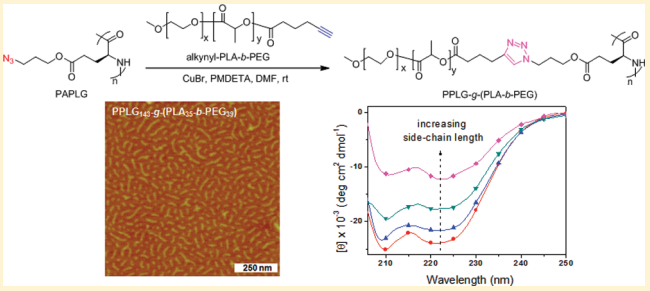

INTRODUCTION

Molecular bottlebrushes are an interesting macromolecular architecture comprised of a linear backbone and densely grafted side chains.[1,2] The backbones of molecular bottlebrushes are in an extended conformation that results from steric repulsions between the side chains, giving rise to interesting physical properties (e.g., shape persistency,[1,2] hindered entanglement,[3,4] promoted ordering to form large domain structures).[5−7] Molecular bottlebrushes have gained increasing attention for potential applications that range from nanotechnology (e.g., photonic crystals,[5−7] nanotubes,[8] and nanowires[9] precursors) to biomedical applications (e.g., drug delivery carriers).[10,11] A variety of homo- and copolymer bottlebrushes with single-component or core−shell side chains have been synthesized by grafting-from,[12] grafting-to,[13] and grafting-through methods with varying degrees of grafting efficiency.[14]

Stimuli-responsive polymers undergo conformational transitions induced by environmental changes such as pH, temperature, light, electric, or magnetic fields.[15−17] The bottlebrush architecture is less explored for the design and synthesis of stimuli-responsive materials.[18] Combining their unique architecture with stimuli-responsive properties will not only allow for direct visualization of externally induced conformational transitions[1,2] but also enable new applications such as photonic-crystal sensors or actuators and smart drug delivery systems.[6,7,18] For example, Schmidt et al. reported the synthesis of thermoresponsive molecular bottlebrushes having poly(*N*-isopropylacrylamide) (PNIPAM) side chains. These polymers change from a cylindrical to a spherical shape in a 18 °C temperature window (i.e., 20−38 °C) as a result of a conformational transition of the side chain.[19] Matyjaszewski and co-workers reported the synthesis of loosely grafted poly(acrylic acid) (PAA) molecular bottlebrushes that undergo globule-to-extended conformational transitions in aqueous solution as the pH is changed from acidic to basic.[20] In these studies, the stimuli-responsive properties are conferred by the side chains. Molecular bottlebrushes with stimuli-responsive backbone provide another mechanism to control the conformation of molecular bottlebrushes.

Polypeptides are attractive biomimetic materials due to their unique combination of properties, namely biocompatibility,

Received: November 15, 2010
Revised: February 4, 2011
Published: February 25, 2011

capability for forming higher order structures, and conformationally coupled self-assembly in solution and solid state.[21−23] The secondary structures of polypeptides (e.g., α-helices and β-sheets) are stabilized by intra- or intermolecular hydrogen bonds. Hence, the helix-to-coil or sheet-to-coil conformational transition can be induced by pH or temperature changes. Cheng and co-workers have recently reported the synthesis of molecular bottlebrushes with densely grafted polypeptide side chains by combining ring-opening metathesis polymerization (ROMP) and ring-opening polymerization (ROP) in a one-pot reaction.[24] However, the stimuli-responsive behavior of these polymers was not investigated. Spurred by the recent development of polymerization methodologies that enable the controlled synthesis of polypeptides with well-defined structures,[25,26] polypeptide-based materials have moved to the forefront of materials science where many ingenious applications of the materials will continue to emerge.[27−29]

In this contribution, we report the synthesis and characterization of core−shell molecular bottlebrushes based on helical polypeptide backbones and densely grafted polylactide-*b*-poly(ethylene glycol) block copolymers (PLA-*b*-PEG) side chains as well as the study of their conformational dependence on pH and temperature changes. The polymers have been characterized by a combination of spectroscopic, chromatographic, and microscopic techniques (i.e., NMR, SEC, AFM). CD and FTIR analysis reveal that the molecular bottlebrushes retain α-helical conformations in solution and in the solid state. The pH and temperature dependence of their solution conformations has also been investigated by CD.

EXPERIMENTAL SECTION

General Considerations. All air- or moisture-sensitive compounds were handled under a nitrogen atmosphere, either using standard Schlenk-line techniques or in a glovebox. Anhydrous toluene, tetrahydrofuran (THF) and *N*,*N*-dimethylformamide (DMF) were obtained by passing through activated alumina columns or molecular sieves under an argon atmosphere (Innovative Technology, Inc.). PEG-OH (M_n = 2025 g mol^{-1}, PDI = 1.03) was purchased from Sigma-Aldrich and was dried by azeotropic distillation from an anhydrous toluene solution. The polymer MW and PDI were determined by MALDI-TOF MS spectrometry. DL-Lactide was purified by sublimation. All other chemicals were purchased from Sigma-Aldrich and used as received. Poly(γ-azidopropyl-L-glutamate) (PAPLG) was synthesized by a previously reported procedure.[30]

^{1}H and ^{13}C{^{1}H} NMR spectra were recorded on a Bruker AV-400 spectrometer. Chemical shifts are reported in ppm and referenced to the solvent protio impurities and solvent ^{13}C{^{1}H} resonances. FTIR spectra were collected on a Bruker Tensor 27 FTIR spectrometer. Size exclusion chromatography (SEC) was performed using an Agilent 1200 system (Agilent 1200 series degasser, isocratic pump, autosampler, and column heater) equipped with three Phenomenex 5 μm, 300 × 7.8 mm columns [100 Å, 1000 Å, and Linear (2)], Wyatt DAWN EOS multiangle light scattering (MALS) detector (GaAs 30 mW laser at λ = 690 nm), and Wyatt Optilab rEX differential refractive index (DRI) detector with a 690 nm light source. DMF containing 0.1 M LiBr was used as the eluent at a flow rate of 0.5 mL min^{-1}. The column temperature was 50 °C, and the detector temperature was 25 °C for both MALS and DRI detectors.

CD data were collected with the high tension voltage (i.e., the voltage applied to the photomultiplier) less than 600 V on a Jasco J810 CD spectrometer (Japan Spectroscopic Corp.) with a path length of 0.1 cm and a bandwidth of 1 nm. Two scans were conducted and averaged between 185 and 250 nm at a scanning rate of 20 nm min^{-1} with a resolution of 0.5 nm. The data were processed by subtracting the solvent background and smoothing with means−movement method with a convolution width ranging from 5 to 25. The CD spectra were reported in mean residue ellipticity (MRE) (units: deg cm^2 dmol^{-1}) which was calculated by the equation $[\theta]_\lambda$= MRW × θ_λ/(10 × d × c),[31] where MRW is the mean residue weight [MRW = (MW of PAPLG repeating unit) + (MW of alkynyl-PLA-*b*-PEG) × grafting density], θ_λ is the observed ellipticity (deg) at the wavelength λ, d is the path length, and c is the concentration (g mL^{-1}).

The following is a representative preparation procedure for CD measurement of the molecular bottlebrush aqueous solutions. The polymer (10.0 mg) was dissolved in THF (2 mL) at room temperature and left overnight. The solution was added dropwise into vigorously stirred distilled water (10 mL). The THF was allowed to evaporate over a period of 48 h at room temperature while maintaining the vigorous stirring. The solution was transferred to a volumetric flask (10 mL) and diluted with additional distilled water. For temperature-dependent CD studies, the solution was allowed to equilibrate for 5 min prior to data collection. For pH-dependent CD studies, the solution pH was adjusted by the addition of aqueous HCl or KOH.

A representative procedure for AFM sample preparation is given as follows. Molecular bottlebrushes in a dilute chloroform solution were deposited on double-distilled water (Mili-Q) in Langmuir−Blodgett trough (KSV 5000). The film was transferred onto a mica substrate at a constant pressure of 1 mN m^{-1} with a transfer ratio of 0.99. AFM images were obtained using a Multimode Nanoscope IIIa atomic force microscope (Veeco Metrology Group) in tapping mode. The molecular weight distribution of the synthesized molecular bottlebrushes was measured by AFM according to a literature method.[32]

Synthesis of Polylactide-*b*-poly(ethylene glycol) (PLA-*b*-PEG). A representative experimental procedure is given as follows. A hot round-bottomed flask (25 mL) was treated with $(CH_3)_2SiCl_2/CH_2Cl_2$ (1.0 M) and baked in an oven at 150 °C overnight prior to use in the reaction. Inside the glovebox, a measured volume of $AlEt_3$/toluene solution (156 μL, 0.0825 mmol, 0.5 M) was added to a PEG-OH (0.25 g, 0.165 mmol)/toluene solution (6 mL) at room temperature. The solution was stirred for 2 h at room temperature. DL-Lactide (0.48 g, 3.3 mmol) was added to the solution, and the mixture was stirred at 90 °C for another 2 h. The reaction cooled to room temperature and quenched by the addition of HCl/methanol solution (0.4 mL, 1.25 M). The reaction mixture was filtered, and the solvent was evaporated under vacuum to yield the crude product. Additional purification by extraction into hot hexanes (60 mL × 6) followed by vacuum drying at 60 °C for 8 h afforded a white solid (0.62 g, 90% yield). (Note: immediately prior to further chain-end derivation, PLA-*b*-PEG was dried by azeotropic distillation from an anhydrous toluene solution.) ^{1}H NMR ($CDCl_3$, δ, ppm): 5.10−5.20 (m, 1H, −C*H*CH$_3$ of PLA), 3.64 (s, 4H, −C*H*$_2$C*H*$_2$− of PEG), 3.38 (s, 3H, end group of C*H*$_3$O−), 1.50−1.60 (m, 3H, −CHC*H*$_3$ of PLA). ^{13}C{^{1}H} NMR ($CDCl_3$, δ, ppm): 169.55, 72.11, 70.74, 69.36, 64.61, 59.23, 20.71, and 16.93. FTIR (neat, cm^{-1}): 2872, 1750, 1452, 1184, and 1082.

Synthesis of Polylactide-*b*-poly(ethylene glycol) Terminated with Alkynyl Functionality (Alkynyl-PLA-*b*-PEG). A $CHCl_3$ (20 mL) solution of 5-hexynoic acid (1.0 g, 8.92 mmol) and thionyl chloride (6.5 mL, 89 mmol) was heated at reflux under nitrogen for 5 h. The solvent and excess thionyl chloride was removed by rotary evaporation at 40 °C to yield a brown oily residue (0.94 g, 81% yield). (Note: to facilitate the complete removal of unreacted thionyl chloride, the brown residue was mixed with hexane and the volatiles evaporated under vacuum. The procedure was repeated several times.) The oily product was used in subsequent reactions without further purification.

Hexynoic acid chloride (0.28 g, 2.1 mmol)/anhydrous THF (5 mL) was slowly added to a THF solution (20 mL) of PLA-*b*-PEG (0.90 g, 0.21 mmol) and anhydrous pyridine (0.2 mL, 2.1 mmol) at 0 °C. The reaction mixture was stirred at room temperature for 24 h and filtered to

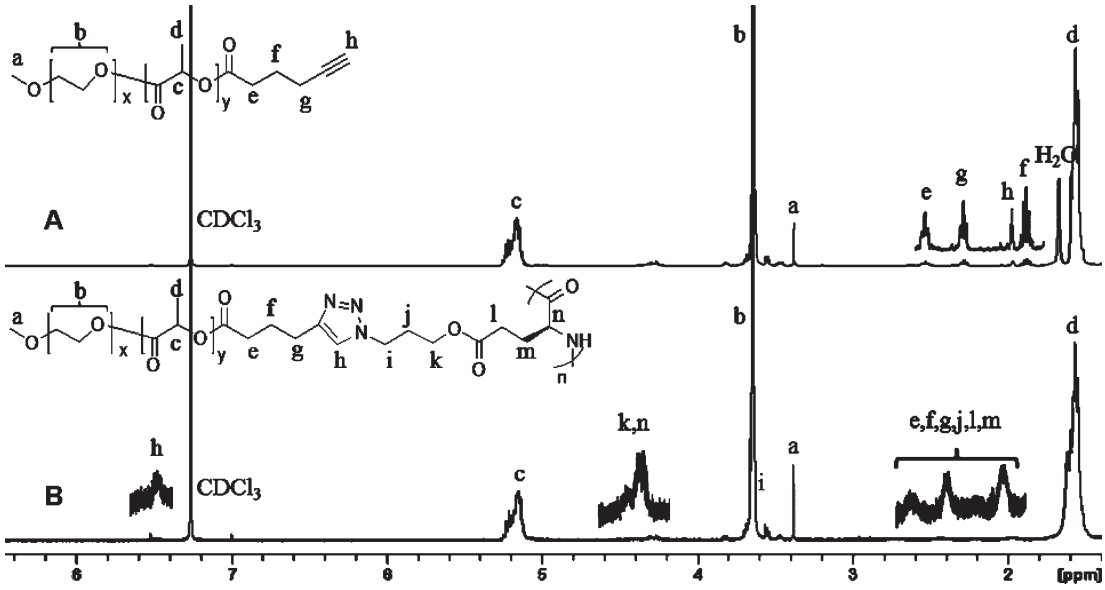

Figure 1. ^{1}H NMR spectra of (A) alkynyl-PLA$_{35}$-*b*-PEG$_{39}$ and (B) PPLG$_{143}$-*g*-(PLA$_{35}$-*b*-PEG$_{39}$) in $CDCl_3$.

remove the insoluble salts. Evaporation of THF under vacuum at 40 °C yielded a yellow glassy solid. Further purification by washing with hot hexane (60 mL × 6) and drying at 60 °C under vacuum for 8 h afforded the final product as a yellow glassy solid (0.75 g, 83% yield). ^{1}H NMR ($CDCl_3$, δ, ppm): 5.10−5.20 (m, 1H, −C*H*CH$_3$ of PLA), 3.64 (s, 4H, −C*H*$_2$C*H*$_2$− of PEG), 3.38 (s, 3H, end group of C*H*$_3$O−), 2.53 (t, 2H, end group of −OOCC*H*$_2$CH$_2$CH$_2$C≡CH), 2.31 (t, 2H, end group of −OOCCH$_2$CH$_2$C*H*$_2$C≡CH), 1.97 (s, 1H, end group of −OOCCH$_2$CH$_2$CH$_2$C≡C*H*), 1.85 (p, 2H, end group of −OOCCH$_2$C*H*$_2$CH$_2$C≡CH), 1.50−1.60 (m, 3H, −CHC*H*$_3$ of PLA). ^{13}C{^{1}H} NMR ($CDCl_3$, δ, ppm): 169.54, 72.11, 70.74, 69.35, 64.60, 59.21, 53.63, 32.69, 23.70, 17.91, and 16.92. FTIR (neat, cm^{-1}): 2872, 1750, 1452, 1184, and 1082.

Synthesis of Core−Shell Molecular Bottlebrushes [PPLG-*g*-(PLA-*b*-PEG)]. Inside the glovebox, CuBr (12 mg, 0.08 mmol) was added to a DMF (10 mL) solution of alkynyl-PLA-*b*-PEG (0.35 g, 0.08 mmol, M_n = 4200 g mol^{-1}, PDI = 1.03), PAPLG (17 mg, 0.08 mmol repeating units, absolute M_n = 30.4 kg mol^{-1}, PDI = 1.19), and PMDETA (18 μL, 0.08 mmol). The reaction mixture was stirred at room temperature for 24 h and quenched by exposure to air. The DMF was vacuum distilled at 60 °C to yield a deep green polymer which was purified by passing through a neutral alumina column using THF as the eluent (R_f = 0.78). Evaporation of the solvent afforded a yellow glassy solid as the final product (0.28 g, 77% yield). ^{1}H NMR ($CDCl_3$, δ, ppm): 7.49 (s, 1H, =C*H*N$_3$−), 5.10−5.20 (m, 1H, −C*H*CH$_3$ of PLA), 4.20−4.40 (m, 3H, −OCH*H*$_2$CH$_2$CH$_2$−triazole and −COC*H*NH−), 3.64 (s, 4H, −C*H*$_2$C*H*$_2$− of PEG), 3.38 (s, 3H, end group of C*H*$_3$O−), 1.90−2.80 (m, 12H, −OOCC*H*$_2$CH$_2$CH$_2$−triazole, −OCHH$_2$C*H*$_2$CH$_2$−triazole and −COCH$_2$CH$_2$CH−), 1.50−1.60 (m, 3H, −CHC*H*$_3$ of PLA). ^{13}C{^{1}H} NMR ($CDCl_3$, δ, ppm): 169.49, 72.09, 69.35, 64.57, 59.20, and 16.94. FTIR (neat, cm^{-1}): 2872, 1750, 1650, 1549, 1452, 1184, and 1082.

The grafting density was calculated by SEC analysis of the relative intensity of PLA-*b*-PEG side-chains before (I_0, peak intensity of PEG-*b*-PLA at time zero) and after click reactions (I_{24}, peak intensity of PEG-*b*-PLA at 24 h, Figure S1). Grafting density = $(I_0 - I_{24})/I_0 \times 100\%$. (Note: reaction aliquots were directly used in the SEC tests without any purification.)

RESULTS AND DISCUSSION

Synthesis of Core−Shell Molecular Bottlebrushes with Helical Polypeptide Backbone. Core−shell molecular bottlebrushes based on polypeptide backbone and polylactide-*b*-poly(ethylene glycol) block copolymer side chains (PLA-*b*-PEG) have been synthesized by a "grafting-to" approach. PLA-*b*-PEG side chains (Figure 1A) have been prepared by metal-mediated ring-opening polymerization of DL-lactide using hydroxyl-terminated PEG (M_n = 2025 g mol^{-1}, PDI = 1.03) as macroinitiator and $AlEt_3$ as catalyst (Scheme 1).[33] The PEO block length was held constant, and the PLA block length was varied to allow for adjustment of the side-chain molecular weight. Their polymer molecular weights have been determined by integrating the PLA and PEO ^{1}H NMR resonances against the methoxy end group. The molecular weight distributions (PDIs) have been determined by SEC, which was calibrated with polystyrene standards. Polymerization occurred in a controlled manner and allowed for ready access to PLA-*b*-PEG having controlled polymer molecular weight (M_n = 2.4−9.8 kg mol^{-1}) and narrow molecular weight distribution (PDI = 1.02−1.03) (Table 1). The block copolymer was quantitatively derivatized via esterification to yield PLA-*b*-PEG bearing an alkynyl functionality at the chain end (alkynyl-PLA-*b*-PEG), as evidenced by the 3:2 integration ratio of the methoxy (a, Figure 1A) and methylene (g, Figure 1A) groups in the ^{1}H NMR spectra. Polypeptide backbones having the azido functionality on the side chains [i.e., poly(γ-azidopropyl-L-glutamate (PAPLG)] were prepared by a published procedure.[30] In the synthesis of the molecular bottlebrushes, the PAPLG segment length was kept constant (absolute M_n = 30.4 kg mol^{-1}, PDI = 1.19). Covalent assembly of the polypeptide backbones and alkynyl-PLA-*b*-PEG side chains was effected by click chemistry (i.e., copper-mediated alkyne−azide [2 + 3] 1,3-dipolar cycloaddition) with the ratio of alkyne to azide groups kept constant at 1:1 to yield the desired molecular bottlebrushes [PPLG-*g*-(PLA-*b*-PEG)] with moderate to high grafting density (82−93%) under mild conditions (Scheme 1). The high grafting density presumably originates from the helical polypeptide backbone conformations that alleviate steric repulsions between the side chains. This is in contrast to molecular bottlebrushes based on random-coil polymer backbones where the grafting density of the polymeric side chain by the "graft-to" approach is typically in the low to

Table 1. $AlEt_3$-Mediated Ring-Opening Polymerizations (ROP) of DL-Lactide Using PEG-OH Macroinitiators

entry	$[M]_0$:$[PEG-OH]_0$ [a]	M_n [b] $\times 10^{-3}$ (g mol^{-1})	M_n [c] $\times 10^{-3}$ (g mol^{-1})	M_n [d] $\times 10^{-3}$ (g mol^{-1})	PDI[d]	conversion[c] (%)	yield (%)
1	5	2.6	2.4	11.9	1.02	84	96
2	20	4.5	4.2	17.0	1.03	86	90
3	40	6.3	6.5	22.7	1.03	75	93
4	80	10.0	9.8	34.6	1.03	69	90

[a] $[PEG\text{-}OH]_0$:$[AlEt_3]_0$ = 2:1, ROP of DL-lactide ($[M]_0$ = 0.54 M) was carried in toluene at 90 °C for 2 h. [b] Theoretical molecular weight. [c] Determined from ^{1}H NMR spectroscopy. [d] Determined from SEC, using PS as the standard.

Scheme 1

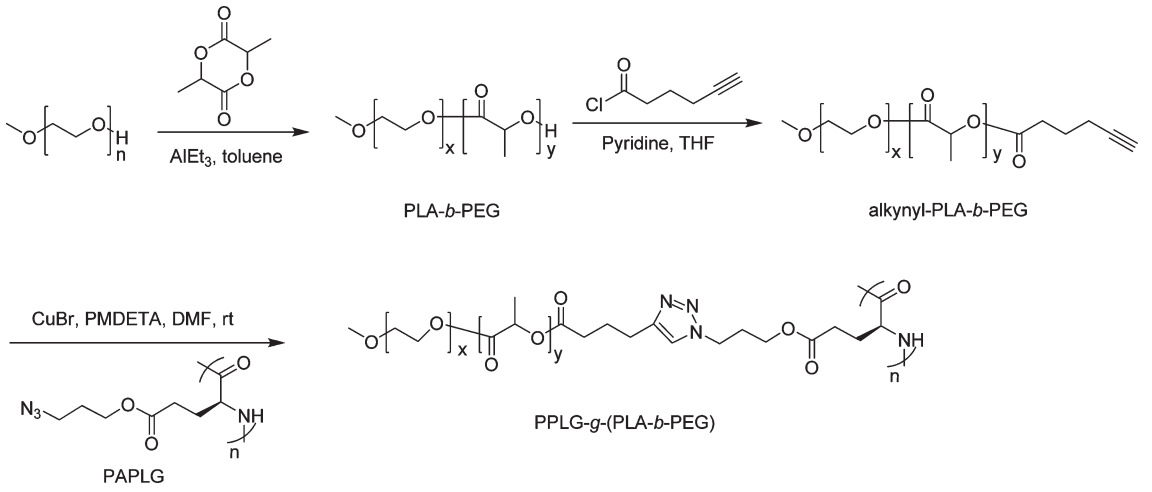

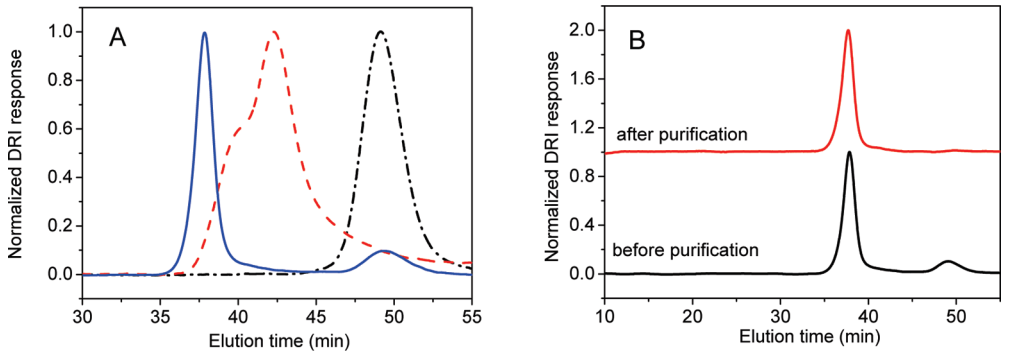

Figure 2. SEC chromatographs of (A) PLA_{35}-*b*-PEG_{39} (— · —) $PAPLG_{143}$ (— — —) and $PPLG_{143}$-*g*-(PLA_{35}-*b*-PEG_{39}) (—) and (B) $PPLG_{143}$-*g*-(PLA_{35}-*b*-PEG_{39}) before and after purification (SEC conditions: 50 °C, 0.1 M LiBr/DMF).

moderate range (<80%), especially when the side chains are bulky.[1,2]

The successful synthesis of the molecular bottlebrushes was verified by ^{1}H NMR (Figure 1B) and SEC techniques (Figure 2A). The relatively low content of the polymeric backbones in the bottlebrush architectures prohibits a reliable assessment of grafting densities by ^{1}H NMR analysis. We hence determined the grafting densities by comparing the relative intensity of the SEC chromatograph peaks due to alkynyl-PLA-*b*-PEG before and after the "click" reactions (Figure S1, Table 2). While we have previously demonstrated that small molecular moieties (e.g., monosaccharide) can be quantitatively grafted onto PAPLG side chains,[30] the grafting densities of the molecular bottlebrush PPLG-*g*-(PLA-*b*-PEG) are lower, presumably due to the greater steric repulsion between the polymeric side chains. Indeed, we have observed an inverse correlation between the grafting density and the molecular size of the diblock copolymer side chains (Table 2).

To further confirm the successful synthesis of the molecular bottlebrushes and independently assess the grafting density, the synthesized polymers were examined by atomic force microscopy (AFM). Figure 3A shows individual molecules of $PPLG_{143}$-*g*-(PLA_{35}-*b*-PEG_{39}) within a dense monolayer prepared by the Langmuir—Blodgett technique. The imaged macromolecules reveal a wormlike conformation with a number-average contour length of L_n = 36.1 ± 1.0 nm. The length value was verified for different substrates to exclude the adsorption-induced rupture of brushlike macromolecules.[34] Since the number-average degree of polymerization for the polypeptide backbone is N_n = 143, the average length per monomeric unit

Table 2. Compositional Parameters of PPLG-*g*-(PLA-*b*-PEG) Molecular Bottlebrushes

molecular bottlebrush composition	grafting density (%)[a]	M_n of PLA-*b*-PEG (kg mol^{-1})[b]	M_w/M_n of PLA-*b*-PEG[c]	$M_n \times 10^{-2}$ (kg mol^{-1})[d]	M_w/M_n[e]	yield (%)
$PPLG_{143}$-*g*-(PLA_9-*b*-PEG_{39})	93	2.4	1.02	3.6	1.14	84
$PPLG_{143}$-*g*-(PLA_{35}-*b*-PEG_{39})	89	4.2	1.03	5.8	1.18	77
$PPLG_{143}$-*g*-(PLA_{66}-*b*-PEG_{39})	88	6.5	1.03	8.6	1.15	81
$PPLG_{143}$-*g*-(PLA_{112}-*b*-PEG_{39})	82	9.8	1.03	11.9	1.26	84

[a] Calculated from SEC by comparing the relative intensity of PLA-*b*-PEG side chains before and after click reaction. [b] Diblock copolymer molecular weights were determined by ^{1}H NMR. [c] Diblock copolymer molecular weight distribution (PDI) were determined from SEC (0.1 M LiBr/DMF) using polystyrene standards. [d] Bottlebrush molecular weights were calculated from the M_n of the main chain plus the M_n of the 5-hexynyl-terminated side-chain × 143 × grafting density. [e] Bottlebrush molecular weight distribution (PDI) were determined from SEC-MALS-DRI (0.1 M LiBr/DMF).

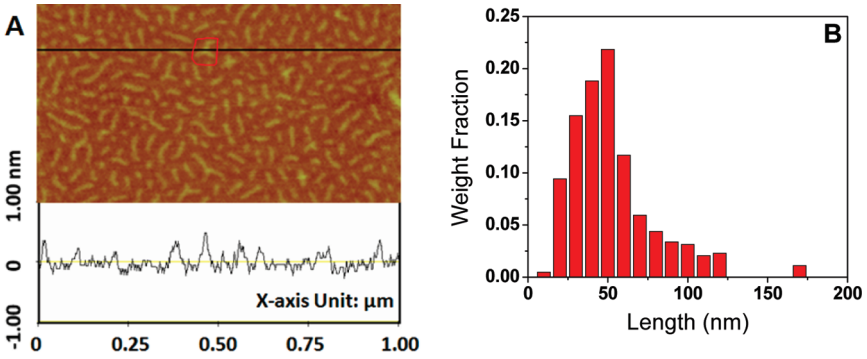

Figure 3. (A) AFM image of $PPLG_{143}$-*g*-(PLA_{35}-*b*-PEG_{39}) and (B) the molecular length distribution measured by AFM for an ensemble of 448 molecules.

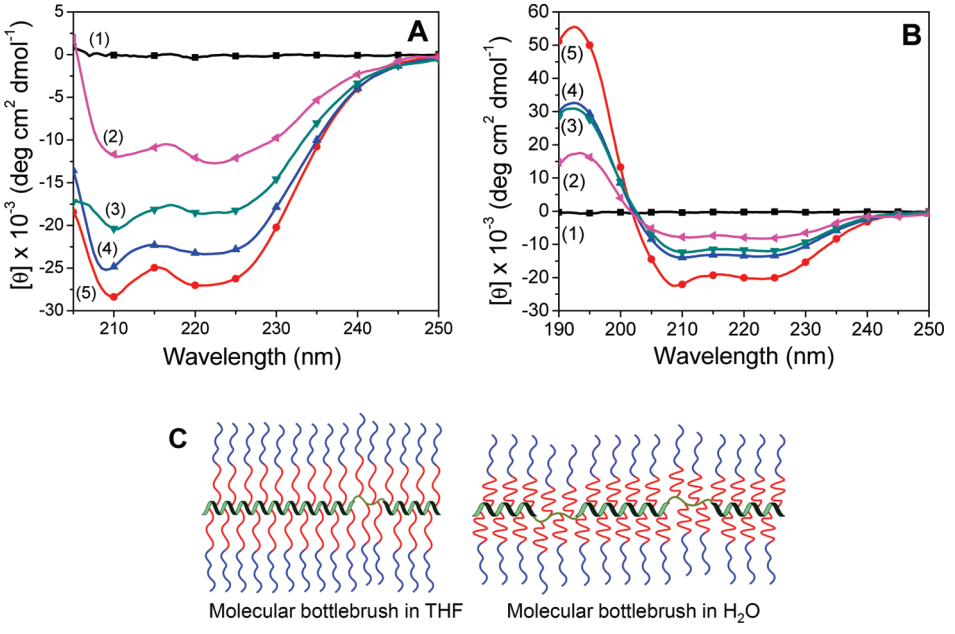

Figure 4. CD spectra of PLA_9-*b*-PEG_{39} (1), $PPLG_{143}$-*g*-(PLA_{112}-*b*-PEG_{39}) (2), $PPLG_{143}$-*g*-(PLA_{66}-*b*-PEG_{39}) (3), $PPLG_{143}$-*g*-(PLA_{35}-*b*-PEG_{39}) (4), and $PPLG_{143}$-*g*-(PLA_9-*b*-PEG_{39}) (5) in THF (A) and in water (B) at 20 °C. (C) Cartoon of the proposed structures of PPLG-*g*-(PLA-*b*-PEG) in THF and in water.

$l_0 = L_n/N_n = 0.25 \pm 0.01$ nm is therefore shorter than the theoretical length of polypeptide backbones adopting zigzag (l_0^{zz} = 0.36 nm) or pleated sheet (l_0^{sheet} = 0.30 nm) conformations but longer than that of α-helices (l_0^{helix} = 0.15 nm). This is consistent with the bottlebrush backbones adopting a stretched helical conformation in the solid state (assuming that N_n is measured correctly). In agreement with this, FTIR analysis of the solid sample reveals amide I and amide II bands at 1650 and 1549 cm^{-1}, respectively, characteristic of polypeptide α-helices (Figure S2).[35]

The combination of the AFM and Langmuir−Blodgett (LB) techniques was also used to characterize the molecular weight (MW) distribution (including M_n and PDI = M_w/M_n).[32] The determined number-average MW ($M_n = 4.3 \times 10^5$ kg mol^{-1}) is

dx.doi.org/10.1021/ma1025994 |*Macromolecules* 2011, 44, 1491–1499

lower than that measured by the SEC-^{1}H NMR method (M_n = 5.8 × 10^5 kg mol^{-1}). The polydispersity index of the molecular bottlebrush length distribution (PDI = 1.33) obtained by AFM analysis (Figure 3B) is larger than that determined by SEC-MALS-DRI analysis (M_w/M_n = 1.18). The discrepancy may in part result from the less representative statistics of AFM analysis.

Conformational Study of Core−Shell Molecular Bottlebrushes. *Solvent Dependence of Molecular Bottlebrush Conformations.* Circular dichroism has been used to examine the secondary structures of the molecular bottlebrushes in solution (i.e., THF and water). The PLA-*b*-PEG block copolymers exhibit no Cotton effect between 190 and 250 nm in either solvent (Figure 4). By contrast, the CD spectra of the molecular bottlebrushes [PPLG-*g*-(PLA-*b*-PEG)] in THF exhibit two negative dichroic bands at 222 and 208 nm which are characteristic of polypeptides α-helical conformations, arising from n−π^* and parallel-polarized $\pi-\pi^*$ excitonic transitions, respectively.[36]

Table 3. Mean Residual Ellipticity ($[\theta]_{222}$) and Fractional Helicity (f_H) of PPLG-*g*-(PLA-*b*-PEG)

	$[\theta]_{222}$		f_H (%)	
sample name	THF[a]	H_2O[a]	THF[a]	H_2O[a]
$PPLG_{143}$-*g*-(PLA_9-*b*-PEG_{39})	−27 001	−20 329	75	62
$PPLG_{143}$-*g*-(PLA_{35}-*b*-PEG_{39})	−23 346	−13 673	65	38
$PPLG_{143}$-*g*-(PLA_{66}-*b*-PEG_{39})	−18 533	−11 918	51	33
$PPLG_{143}$-*g*-(PLA_{112}-*b*-PEG_{39})	−12 692	−8 235	35	23

[a] CD spectra were collected with a polymer concentration of 2.0 and 1.0 mg mL^{-1} in THF and H_2O, respectively.

The perpendicularly polarized $\pi-\pi^*$ excitonic transition at about 190 nm, which is also characteristic of the polypeptide α-helical conformation, is not observed in THF due to solvent absorption at this wavelength. The transition is observed when the CD spectra are collected in aqueous solution (Figure 4B). The CD spectra are identical at different polymer concentrations (0.5−2.0 mg mL^{-1} in THF and 0.5−1.0 mg mL^{-1} in water), suggesting minimal or no aggregation under the experimental conditions. Further reduction in the polymer concentration to below 0.5 mg mL^{-1} results in noisy and unreliable CD spectra.

To allow for comparison of the relative helical conformation content in our molecular bottle brushes with variable side-chain lengths at different pH and temperature, we calculated the fractional helicity (f_H) (eq 1):

$$f_H = \frac{[\theta]_{222}}{-37000(1 - 2.6/n)} \quad (1)$$

where $[\theta]_{222}$ is the mean residue ellipticity at 222 nm and n is the average degree of polymerization for the polypeptide backbones.[37]

The f_H decreases with increasing side-chain length, which is attributed to the increased steric repulsion between side chains that destabilizes the helical backbone conformation. All molecular bottlebrush samples exhibit lower f_Hs in water (23−62%) than in THF (35−75%) (Table 3). The solvent-dependent polypeptide backbone helicity may arise from the complex interplay of several contributing factors. For example, while THF and water are both good solvents for PEO, PLA is readily soluble in THF but not in water. This gives rise to appreciably different PLA conformations in the proximity of the polypeptide

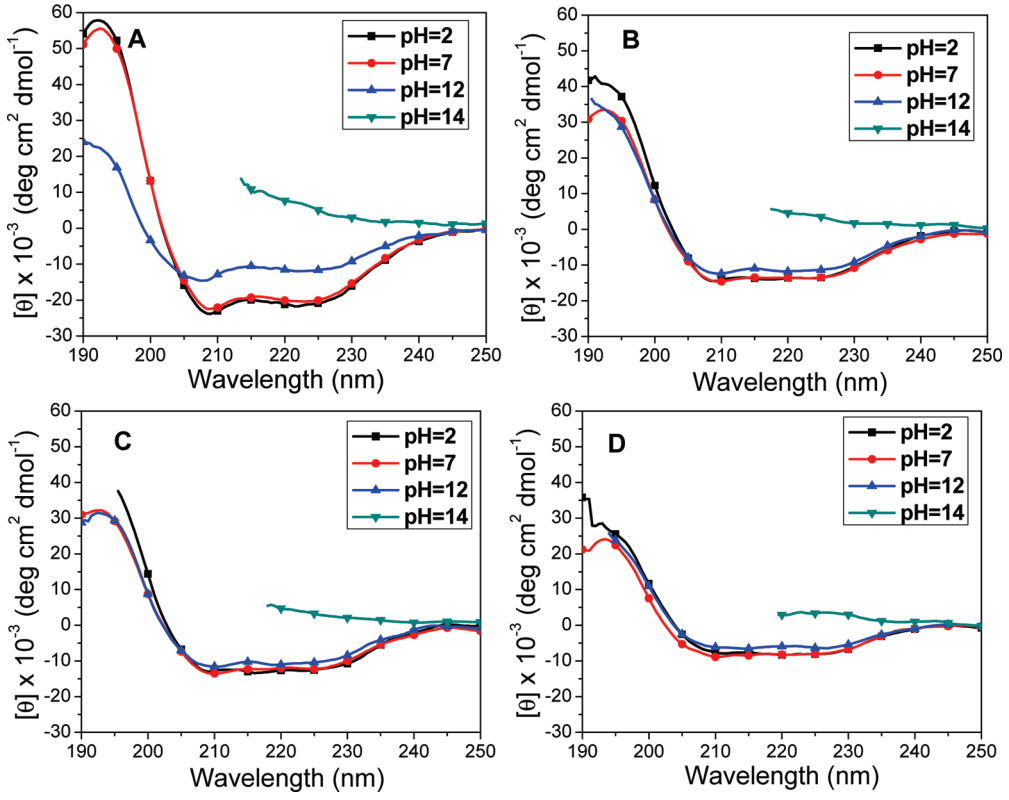

Figure 5. CD spectra of molecular bottlebrushes of variable side-chain lengths: (A) $PPLG_{143}$-*g*-(PLA_9-*b*-PEG_{39}), (B) $PPLG_{143}$-*g*-(PLA_{35}-*b*-PEG_{39}), (C) $PPLG_{143}$-*g*-(PLA_{66}-*b*-PEG_{39}), and (D) $PPLG_{143}$-*g*-(PLA_{112}-*b*-PEG_{39}) in aqueous solutions with different pH at 20 °C (polymer concentration: 1.0 mg·mol^{-1}).

dx.doi.org/10.1021/ma1025994 |*Macromolecules* 2011, 44, 1491–1499

backbone; i.e., the PLA segments adopt an expanded conformation in THF whereas in water the chains collapse into a compact state (Figure 4C). As a result, in THF solvent one would expect enhanced steric repulsion between PLA segments close to the polypeptide backbone and hence a more drastic destabilization of the backbone helical conformation. However, the opposite trend is observed. Another important factor is solvent interaction with the polypeptide backbone. Water is clearly better at hydrogen bonding with polypeptides than THF, and thus water molecules that penetrate the amphiphilic core−shells to the proximity of the polypeptide backbones may cause greater disruption of the helical conformations through intermolecular hydrogen-bonding interactions, hence resulting in reduced fractional helicities as compared with THF solvent. Partial solvation of the PLA segments by water is evidenced by the presence of PLA resonances in ^{1}H NMR spectra in D_2O (Figure S4). By contrast, complete phase segregation of PLA segments would result in substantial reduction or disappearance of the PLA ^{1}H resonances.[38]

pH Dependence of Molecular Bottlebrush Conformations. Poly(L-glutamic acid) (PLGA) and poly(L-lysine) (PLL) are polypeptides whose pH-responsive behavior is well studied. PLGAs adopt α-helical conformations at low pH (i.e., pH ≤ 6.3),[39,40] while PLLs become α-helical at high pH (i.e., pH ≥ 8.4).[41] The pH-induced coil-to-helix transitions arise from the altered the charge density on the polypeptide side chains.[42,43] Increasing the charge density on the side chains destabilizes the α-helical conformations through increased electrostatic repulsion.

CD analysis of the molecular bottlebrush samples [i.e., $PPLG_{143}$-*g*-(PLA_n-*b*-PEG_{39}), n = 9, 35, 66, 112] reveals intriguing pH- and temperature-induced conformational changes in the polypeptide backbones. In aqueous solution, the molecular bottlebrushes adopt reasonably stable α-helical conformations under acidic or neutral conditions (pH = 2 or 7), becoming increasingly unstable and eventually unfolding as the solution becomes basic (Figure 5). For example, while the fractional helicity of $PPLG_{143}$-*g*-(PLA_9-*b*-PEG_{39}) decreases by only 5% from pH 2 to pH 7 (Table S1, entries 1 and 2), on increasing to pH 12, f_H exhibits a significant decrease of 42% (Table S1, entry 3). At pH 14, a complete helix to random coil transition occurs, as manifested by complete disappearance of the dichroic band with negative ellipticity at 220 nm (Figure 5A and Table S1, entry 4). As PLAs are particularly susceptible to hydrolysis under basic conditions, the polymer brushes that have been studied by CD in aqueous solutions of different pH were isolated and re-examined for structural changes. SEC and ^{1}H NMR analysis has verified that hydrolysis of the PLA and the side-chain γ-ester linkages occurs under basic conditions (Figure S3), resulting in the formation of poly(L-glutamic acid), which is observed in the CD spectra at pH 12 and 14. Under the conditions of the CD studies, the bottlebrush structure remains intact in the pH range 2−7.

All molecular bottlebrush samples with different side-chain lengths exhibit similar trends in the pH-dependent CD analysis (Figure 5), i.e., stable α-helical conformations at pH ≤ 7 and random-coil conformations at pH 14 due to formation of poly(L-glutamic acid) by side-chain degradation (Figure S3). As the pH is increased from 7 to 12, the bottlebrushes with longer side chains [i.e., $PPLG_{143}$-*g*-(PLA_n-*b*-PEG_{39}), n = 35, 66, 112] display a less appreciable reduction in fractional helicity than the ones with the shortest side chains [i.e., $PPLG_{143}$-*g*-(PLA_9-*b*-PEG_{39})].

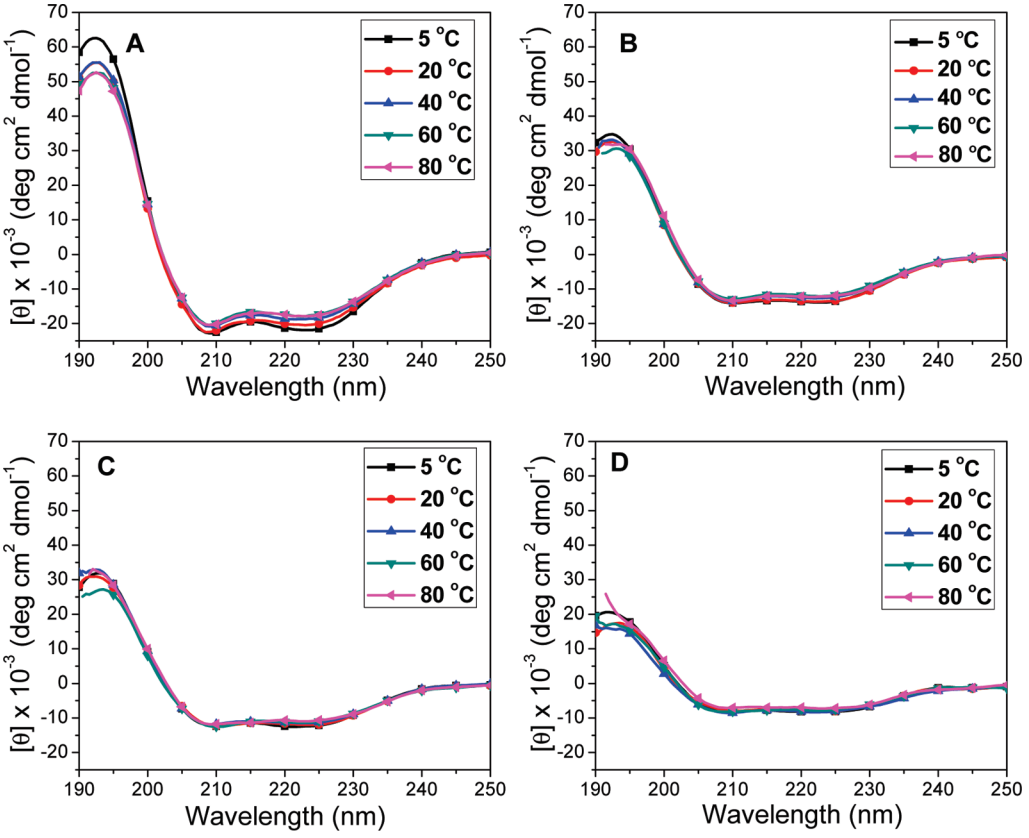

Figure 6. CD spectra of (A) $PPLG_{143}$-*g*-(PLA_9-*b*-PEG_{39}), (B) $PPLG_{143}$-*g*-(PLA_{35}-*b*-PEG_{39}), (C) $PPLG_{143}$-*g*-(PLA_{66}-*b*-PEG_{39}), and (D) $PPLG_{143}$-*g*-(PLA_{112}-*b*-PEG_{39}) in aqueous solutions (pH = 7) at different temperatures between 5 and 80 °C (polymer concentration: 1.0 mg·mol^{-1}).

dx.doi.org/10.1021/ma1025994 |*Macromolecules* 2011, 44, 1491–1499

This is likely due to incomplete degradation of the PLA side-chains in the former between the time of making the sample and recording the CD spectra (Figure 5 and Tables S1−S4, entries 2 and 3).

Temperature Dependence of Molecular Bottlebrush Conformations. CD spectra of the molecular bottlebrushes with different side-chain lengths [i.e., $PPLG_{143}$-*g*-(PLA_n-*b*-PEG_{39}), n = 9, 35, 66, 112] have also been collected at different temperature in neutral aqueous solution (Figure 6) and in THF solution (Figure S5). Temperature variation can induce partial and reversible unfolding of the helical conformations of the molecular bottlebrush backbones. For example, $PPLG_{143}$-*g*-(PLA_9-*b*-PEG_{39}) exhibits 18% reduction in fractional helicity upon increasing the temperature from 5 to 80 °C (Table S1, entries 5 and 9). The fractional helicity observed at 5 °C is fully recovered once the sample has cooled from 80 °C. The effect of temperature on the fractional helicity becomes less appreciable for molecular bottlebrushes having longer side chains [i.e., $PPLG_{143}$-*g*-(PLA_n-*b*-PEG_{39}), n = 35, 66, 112] (Figure 6B−D). This is likely due to the enhanced steric hindrance of the longer side chains which inhibit helix unfolding.

CONCLUSIONS

We have demonstrated that core−shell molecular bottlebrushes with helical polypeptide backbones and amphiphilic diblock copolymer side chains [PPLG-*g*-(PLA-*b*-PEG)] can be readily synthesized by a "grafting-to" approach using click chemistry. The grafting densities for the side chains are reasonably high (82−93%) and decrease with the size of the polymeric side chains. Through molecular imaging by AFM, we have verified a wormlike conformation of adsorbed macromolecules and provided an independent assessment of the grafting density of the molecular bottlebrushes. CD and FTIR analysis of the molecular bottlebrushes reveal that the polypeptide backbones retain α-helical conformations in solution (i.e., water or THF) and the solid state, which is consistent with the AFM observation of the relatively short molecular brushes. Increasing the side-chain length destabilizes the helical conformations of the backbone, presumably due to increased steric repulsion between the side chains. pH-dependent CD analysis reveals that the helical backbone conformations of the bottlebrushes are stable between pH 2 and 7 in room temperature aqueous solution. Further increase of pH results in rapid degradation of polymeric side chains by ester hydrolysis and the formation of poly(L-glutamic acid). While an increase in temperature causes partial and reversible unfolding of the helical backbones, the effect is greatly diminished for the bottlebrushes with longer side chains, presumably due to the enhanced steric hindrance of the side chains. These amphiphilic core−shell molecular bottlebrushes may be potentially utilized as unimolecular micelles for controlled substance release applications. Efforts toward this goal as well as investigation of their self-assembly properties are currently in progress.

ASSOCIATED CONTENT

Supporting Information. SEC traces of PLA-*b*-PEG and corresponding PPLG-*g*-(PLA-*b*-PEG) in 0.1 M LiBr/DMF solution before and after click reactions (Figure S1), FTIR spectra of $PAPLG_{143}$, alkynyl-PLA_{35}-*b*-PEG_{39}, and $PPLG_{143}$-*g*-(PLA_{35}-*b*-PEG_{39}) in the solid state (Figure S2), representative SEC chromatogram of the degradation polymer products isolated from the PPLG-*g*-(PLA-*b*-PEG) aqueous solution (pH = 12) used in CD measurement (Figure S3), representative ^{1}H NMR spectrum of PPLG-*g*-(PLA-*b*-PEG) in D_2O (Figure S4), CD spectra of the molecular brushes with variable side-chain lengths at different temperature in THF (Figure S5), pH- and temperature-dependent CD analysis of the molecular bottlebrushes with variable side-chain lengths in water (Tables S1−S4) and in THF (Table S5). This material is available free of charge via the Internet at http://pubs.acs.org.

AUTHOR INFORMATION

Corresponding Author
*E-mail: dhzhang@lsu.edu.

ACKNOWLEDGMENT

This work is supported by LSU, Louisiana Board of Regents [LEQSF(2008-11)-RD-A-11] and NSF (CHE 0955820 and DMR 0906985).

REFERENCES

(1) Sheiko, S. S.; Sumerlin, B. S.; Matyjaszewski, K. *Prog. Polym. Sci.* **2008**, *33*, 759–785.
(2) Zhang, M.; Müller, A. H. E. *J. Polym. Sci., Part A: Polym. Chem.* **2005**, *43*, 3461–3481.
(3) Neugebauer, D.; Zhang, Y.; Pakula, T.; Sheiko, S. S.; Matyjaszewski, K. *Macromolecules* **2003**, *36*, 6746–6755.
(4) Bolisetty, S.; Airaud, C.; Xu, Y.; Müller, A. H. E.; Harnau, L.; Rosenfeldt, S. *Phys. Rev. E* **2007**, *75*, 040803.
(5) Runge, M. B.; Bowden, N. B. *J. Am. Chem. Soc.* **2007**, *129*, 10551–10560.
(6) Xia, Y.; Olsen, B. D.; Kornfield, J. A.; Grubbs, R. H. *J. Am. Chem. Soc.* **2009**, *131*, 18525–18532.
(7) Rzayev, J. *Macromolecules* **2009**, *42*, 2135–2141.
(8) Huang, K.; Rzayev, J. *J. Am. Chem. Soc.* **2009**, *131*, 6880–6885.
(9) Djalali, R.; Li, S.-Y.; Schmidt, M. *Macromolecules* **2002**, *35*, 4282–4288.
(10) Du, J.-Z.; Tang, L.-Y.; Song, W.-J.; Shi, Y.; Wang, J. *Biomacromolecules* **2009**, *10*, 2169–2174.
(11) Zhang, W.; Li, Y.; Liu, L.; Sun, Q.; Shuai, X.; Zhu, W.; Chen, Y. *Biomacromolecules* **2010**, *11*, 1331–1338.
(12) Lee, H.; Jakubowshi, W.; Matyjaszewski, K.; Yu, S.; Sheiko, S. S. *Macromolecules* **2006**, *39*, 4983–4989.
(13) Gao, H.; Matyjaszewski, K. *J. Am. Chem. Soc.* **2007**, *129*, 6633–6639.
(14) Jha, S.; Dutta, S.; Bowden, N. B. *Macromolecules* **2004**, *37*, 4365–4374.
(15) Dimitrov, I.; Trzebicka, B.; Mueller, A. H. E.; Dworak, A.; Tsvetanov, V. B. *Prog. Polym. Sci.* **2007**, *32*, 1275–1343.
(16) Hoffman, A. S.; Stayton, P. S. *Prog. Polym. Sci.* **2007**, *32*, 922–932.
(17) Gil, E. S.; Hudson, S. M. *Prog. Polym. Sci.* **2004**, *29*, 1173–1222.
(18) Lee, H.; Pietrasik, J.; Sheiko, S. S.; Matyjaszewski, K. *Prog. Polym. Sci.* **2010**, *35*, 24–44.
(19) Li, C.; Gunari, N.; Fischer, K.; Janshoff, A.; Schmidt, M. *Angew. Chem., Int. Ed.* **2004**, *43*, 1101–1104.
(20) Lee, H.-i.; Boyce, J. R.; Nese, A.; Sheiko, S. S.; Matyjaszewski, K. *Polymer* **2008**, *49*, 5490–5496.
(21) Robinson, C.; Ward, J. C.; Beevers, R. B. *Discuss Faraday Soc.* **1958**, *25*, 29–42.
(22) Tang, H.; Zhang, D. *J. Polym. Sci., Part A: Polym. Chem.* **2010**, *48*, 2340–2350.
(23) Block, H. Poly(γ-benzyl-L-glutamate) and Other Glutamic Acid Containing Polymers. *Polymer Monographs*; Gordon and Breach Science Publisher: New York, 1983; Vol. 9, pp 1−214.

(24) Lu, H.; Wang, J.; Lin, Y.; Cheng, J. *J. Am. Chem. Soc.* **2009**, *131*, 13582–13583.
(25) Deming, T. J. *Adv. Polym. Sci.* **2006**, *202*, 1–18.
(26) Lu, H.; Cheng, J. *J. Am. Chem. Soc.* **2007**, *129*, 14114–14115.
(27) Bellomo, E.; Wyrsta, M. D.; Pakstis, L.; Pochan, D. J.; Deming, T. J. *Nature Mater.* **2004**, *3*, 244–248.
(28) Klok, H.-A. *Macromolecules* **2009**, *42*, 7990–8000.
(29) Rao, J.; Luo, Z.; Ge, Z.; Liu, H.; Liu, S. *Biomacromolecules* **2007**, *8*, 3871–3878.
(30) Tang, H.; Zhang, D. *Biomacromolecules* **2010**, *11*, 1585–1592.
(31) Kelly, S. M.; Jess, T. J.; Price, N. C. *Biochim. Biophys. Acta* **2005**, *1751*, 119–139.
(32) Sheiko, S. S.; da Silva, M.; Shirvaniants, D.; LaRue, I.; Prokhorova, S.; Moeller, M.; Beers, K.; Matyjaszewski, K. *J. Am. Chem. Soc.* **2003**, *125*, 6725–6728.
(33) Wang, Y.; Hillmyer, M. A. *Macromolecules* **2000**, *33*, 7395–7403.
(34) Sheiko, S. S.; Sun, F. C.; Randal, A.; Shirvaniants, D.; Matyjaszewski, K.; Rubinstein, M. *Nature* **2006**, *440*, 191–194.
(35) Fraser, D.; Price, W. *Nature* **1952**, *170*, 490–491.
(36) Sreerama, N.; Woody, R. W. In *Circular Dichroism Principle and Application*, 2nd ed.; Berova, N., Nakanishi, K., Woody, R. W., Eds.; Wiley-VCH: New York, 2000; pp 601−620.
(37) Besley, N. A.; Hirst, J. D. *J. Am. Chem. Soc.* **1999**, *121*, 9636–9644.
(38) Cheng, G.; Böker, A.; Zhang, M.; Krausch, G.; Müller, A. H. E. *Macromolecules* **2001**, *34*, 6883–6888.
(39) Niwa, M.; Morikawa, M.; Higashi, N. *Langmuir* **1999**, *15*, 5088–5092.
(40) Wang, Y.; Chang, Y. C. *Macromolecules* **2003**, *36*, 6503–6510.
(41) Wang, Y.; Chang, Y. C. *Macromolecules* **2003**, *36*, 6510–6518.
(42) Nagasawa, M.; Holtzer, A. *J. Am. Chem. Soc.* **1964**, *86*, 538–543.
(43) Meyer, Y. P. *Macromolecules* **1969**, *2*, 624–628.